Title: The hippocampus binds movements to their temporal position in a motor sequence

Authors: Nina Dolfen[1,2,3], Serena Reverberi[1,2], Hans Op de beeck[2,4], Bradley R. King[5], and Genevieve Albouy[1,2,5*]

Affiliations:

[1] Department of Movement Sciences, KU Leuven, Leuven, Belgium

[2] KU Leuven Brain Institute (LBI), Leuven, Belgium

[3] Department of Psychology, Columbia University, New York City, NY, USA

[4] Department of Brain and Cognition, KU Leuven, Leuven, Belgium

[5] Department of Health and Kinesiology, College of Health, University of Utah, Salt Lake City, UT, USA

***Corresponding author:** Genevieve Albouy

Email: genevieve.albouy@kuleuven.be

Competing Interest Statement: None

Classification: Biological Sciences

Keywords: hippocampus, sequence learning, procedural memory

Abstract

A plethora of daily motor tasks consist of sequences of movements or steps that need to be performed in a specific order. Yet, it remains unclear how the brain represents sequential motor actions in a way that preserves their temporal order. Here, we used multivoxel pattern similarity analysis of functional Magnetic Resonance Imaging (fMRI) data acquired during motor sequence practice to investigate whether the hippocampus, a brain region known to support temporal order in the non-motor memory domain, represents information about the temporal order of sequential motor actions. We also examined such representation in other regions of the motor network (i.e., the premotor cortex (PMC), supplementary motor area (SMA), anterior superior parietal lobule (aSPL) and striatum) known for their critical role in motor sequence learning. Our results show that hippocampal activation patterns carried information about movements in their learned temporal position in the sequence, but not about movements or positions in random movement patterns. A similar pattern of results was observed in the striatum. Our data also indicate that multivoxel patterns in M1, SMA and aSPL carried movement-based information while the PMC represented both movement- and position-based information. Altogether, our findings provide novel insight into the role of the hippocampus in the motor memory domain and point to its capacity to bind movements to their temporal position in a motor sequence. Our results also deepen our understanding of how striatal and cortical regions contribute to motor sequence learning via position and movement coding.

Introduction

Many of our everyday tasks, such as making a cup of tea or coffee, consist of repeated sequences of highly similar motor actions or steps. Learning and remembering the correct order of these motor actions is fundamental for successful task completion. Yet, it remains unclear how the brain encodes and represents sequential motor actions in a way that preserves their order. In the last decade, findings in the non-motor memory domain have indicated that the hippocampus plays a critical role in representing and preserving the order of sequential information (1). Neuroimaging studies revealed that multivoxel patterns of activation in the hippocampus are sensitive to the order of items and contain information about the temporal order of episodic events (2) as well as items in learned sequences (i.e., letters in (3) and objects in (4)). Such hippocampal patterns have also been found to predict subsequent memory of the temporal order of the learned items (2, 5). Importantly, it is currently unknown whether the hippocampus represents information about the order of actions in motor sequences.

Evidence from the motor memory domain shows that the hippocampus is involved in the encoding and consolidation of newly learned motor sequences (6, 7). Hippocampal activity during early learning is thought to support the development of a spatial, effector-independent, representation of the motor sequence that encompasses the goal of the series of movements to be executed (6, 8). Recent research suggests that these hippocampal representations are reactivated during post-encoding offline episodes (9) and are linked to successful motor memory retention (8, 10). Surprisingly, the potential role of the hippocampus in coding the temporal order of movements (i.e., binding movements to their temporal position in a sequence) has only been suggested in a previous behavioral study (11). Here, we used multivoxel pattern similarity analysis of functional Magnetic Resonance Imaging (fMRI) data acquired during motor sequence practice to directly test this hypothesis.

In the current study, participants learned a fixed sequence of eight finger movements through repeated practice. Immediately following learning, participants were scanned while practicing the learned sequential pattern (i.e., motor sequence learning task) as well as random movement patterns (i.e., control task) using the same fingers but pressed in a random order. Given the specific role of the hippocampus in encoding and preserving order in other memory domains (1) and based on evidence that the hippocampus is critical for learning series of movements (6, 7), we predicted that hippocampal activation patterns would carry information about finger movements in their learned position in the sequence (i.e., finger-position binding) above and beyond information about finger movements or positions alone. We also examined such coding in other regions of the motor network (i.e., the premotor cortex (PMC), supplementary motor area (SMA), anterior superior parietal lobule (aSPL) and

striatum) that have recently been implicated in the encoding of sequence order during motor sequence learning (13–15).

Results

As illustrated in Figure 1A, all participants completed a (1) learning, (2) fMRI and (3) retention session during which they performed a serial reaction time task (SRTT). Task instruction was to respond as fast as possible to the location of a cue that appeared on the screen (8 locations, 8 fingers, no thumbs; Fig. S1). Depending on the task condition, the cues either followed a pseudorandom (RND SRTT, control task) or fixed, repeating sequential pattern (SEQ SRTT; motor sequence learning task). The repeating pattern in the SEQ condition consisted of an eight-element sequence of finger movements in which each finger was pressed once. In the RND condition, there was no repeating sequence, but each key was pressed once every eight elements.

Behavioral results

After baseline assessment of motor performance (see Supplementary Results section 1.1), participants performed the SEQ SRTT and learned a sequence of eight finger movements through repeated practice. Behavioural results showed that performance speed (reaction time) and accuracy (% of correct responses) progressively improved across SEQ practice blocks (block; speed: $F_{(2.77,88.858)} = 10.96$, $\eta_p^2 = .255$, $p < .001$; accuracy: $F_{(8.474,271.169)} = 2.011$, $\eta_p^2 = .059$, $p = .042$; Fig. 1B, learning). These results suggest that, as expected, participants learned the sequence of finger movements. The learning session was immediately followed by an fMRI session. To optimize the multivariate analyses of the corresponding MRI data (see details in methods), RND and SEQ SRTT conditions were randomly alternated in each fMRI run. To investigate behavioral changes during the fMRI session, a 2 (condition) by 8 (run) RM ANOVA was performed on both speed and accuracy measures. Performance speed was significantly faster in the SEQ as compared to RND condition (condition: $F_{(1,31)} = 96.089$, $\eta_p^2 = .756$, $p < .001$) and fluctuated similarly across fMRI runs in both conditions (run: $F_{(2.518,78.061)} = 3.246$, $\eta_p^2 = .095$, $p = .034$; run x condition: $F_{(4.882, 151.344)} = .719$, $\eta_p^2 = .023$, $p = .656$; Fig. 1C, fMRI). Performance accuracy was overall higher in the SEQ as compared to the RND condition (condition: $F_{(1,31)} = 26.908$, $\eta_p^2 = .465$, $p < .001$) and remained stable across runs in both conditions (run: $F_{(2.958,91.687)} = .550$, $\eta_p^2 = .017$, $p = .647$; run x condition: $F_{(7, 217)} = .787$, $\eta_p^2 = .025$, $p = .599$; Fig. 1C, fMRI). These results indicate that participants presented a sequence-specific performance advantage in the scanner despite the interleaved nature of practice. Last, results showed a main effect of condition on both speed and accuracy during retention, indicating sequence-specific retention of the skill outside of the scanning environment (condition x block RM ANOVA; condition: speed, $F_{(1,31)} = 199.082$, $\eta_p^2 = .865$, $p < .001$, accuracy, $F_{(1,31)} = 29.727$, $\eta_p^2 = .490$, $p < .001$; all other effects: all ps $\geq .172$).

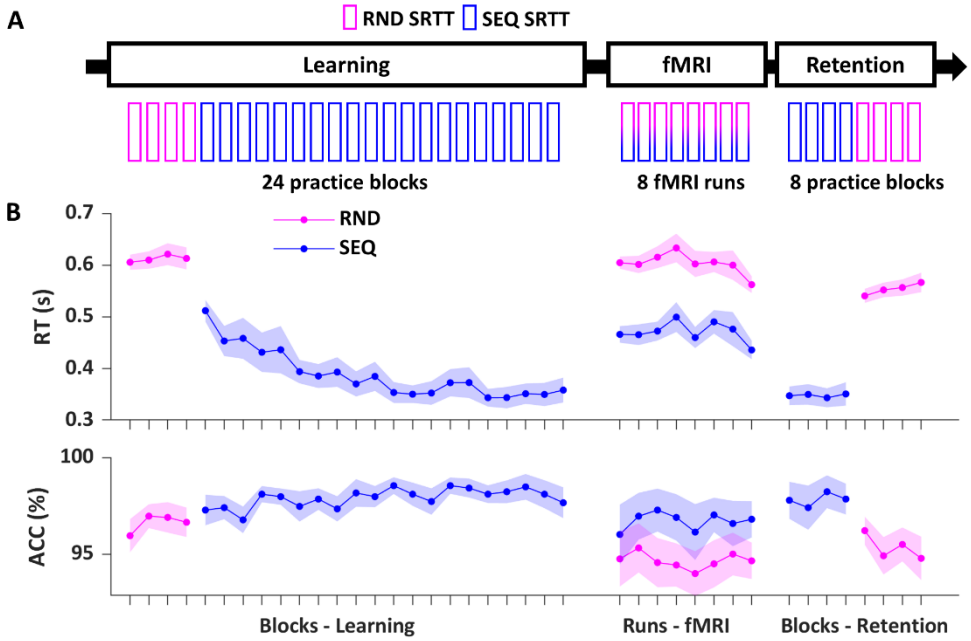

Figure 1 – **(A) General procedure.** All participants completed a learning, fMRI and retention session during which they performed a serial reaction time task (SRTT; see Figure S1). Depending on the task condition, cues in the SRTT followed a random (RND) or repeating, sequential (SEQ) pattern. During the learning and retention sessions, the task took place outside the scanner and was organized in blocks of practice. During the fMRI session, data were acquired over eight consecutive scanning runs during which RND and SEQ SRTT conditions randomly alternated. **(B) Behavioral results for all sessions**. Reaction time (RT; s) and accuracy (ACC; %) for the RND and SEQ SRTT conditions are plotted across blocks of practice for the learning and retention sessions, and across runs for the fMRI session. N = 33. Shaded regions represent SEM.

Neuroimaging results

We used multivoxel pattern similarity analyses of task-related fMRI data to characterize coding of temporal order information during motor sequence learning. Similarity analyses are based on the notion that the relative pattern of activation across voxels in a given brain region is informative about the type of information that is processed by that region (16). Specifically, if a region codes for a particular type of information, higher similarity in voxel activity patterns are expected between pairs of trials sharing this information as compared to pairs of trials not sharing this information. Using this approach, we measured the extent to which specific regions of interest (ROIs) represent information about finger movements in their learned temporal position in the sequence (i.e., finger-position binding). Additionally, to assess the contribution of finger and position coding to the binding described above, we performed control analyses using the random task to test whether the ROIs carried information about (1) finger movements irrespective of their position in the movement pattern (i.e., finger coding), and (2) temporal positions irrespective of the finger movement performed (i.e., position coding). Analyses were performed on seven bilateral ROIs involved in motor sequence learning: the primary motor cortex (M1), the supplementary motor cortex (SMA), the premotor cortex (PMC), the

anterior part of the superior parietal lobule (aSPL), the hippocampus, the putamen, and the caudate nucleus (see regions of interest section in the methods).

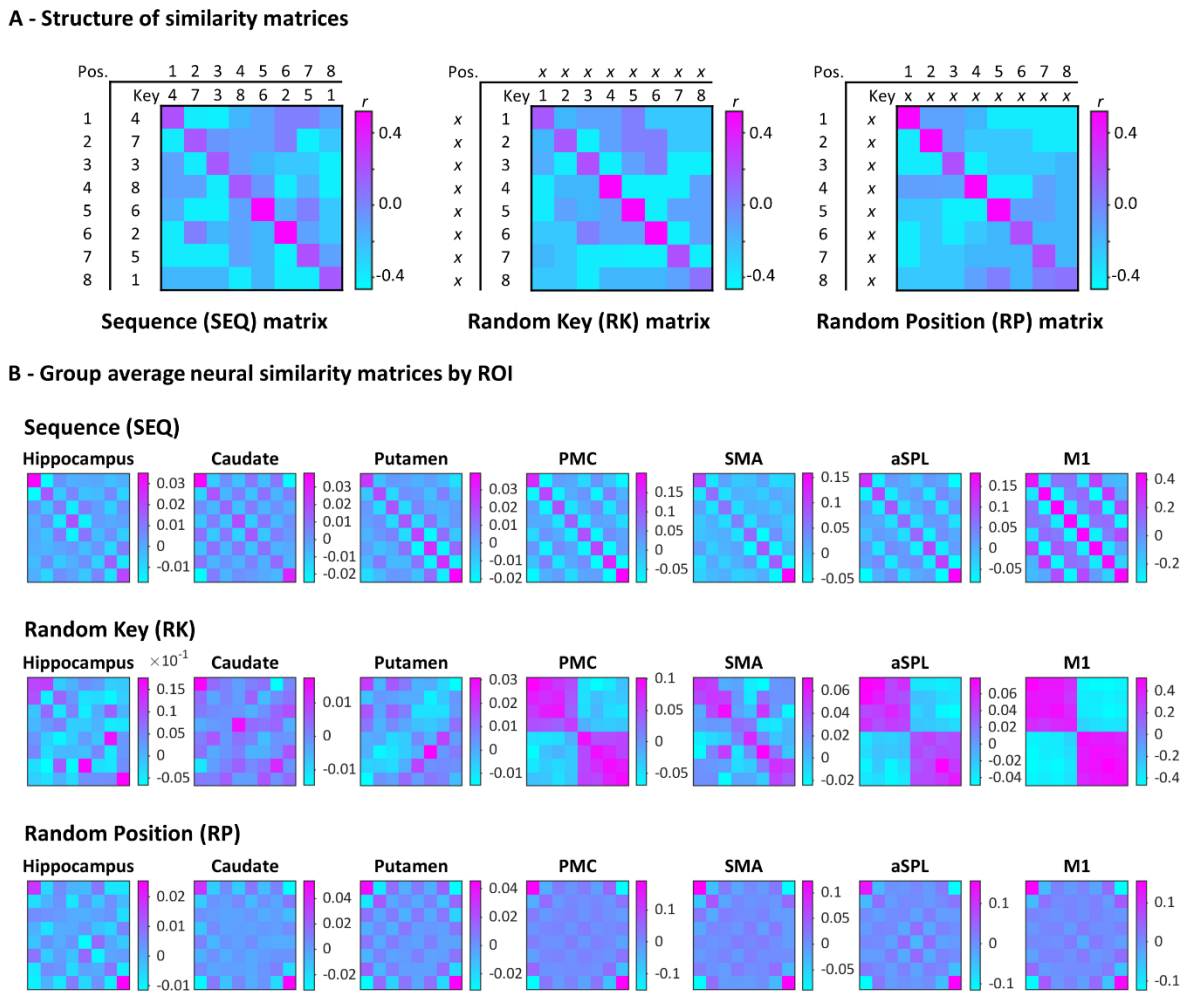

Figure 2. (A) Structure of neural similarity matrices for an exemplary sequence/individual. Pattern similarity was computed across repetitions of the motor sequence to assess finger-position binding in the sequence condition (SEQ matrix) as well as across repetitions of the random patterns to quantify coding of individual finger movements (i.e., key presses; Random Key (RK) matrix) and positions (Random Position (RP) matrix) in the random condition. Pairs of trials sharing a particular type of information (same finger + position, same finger, or same position) are represented on the diagonal of each matrix. In the SEQ matrices, diagonal cells index pattern similarity in activation patterns between the same finger movements sharing the same temporal position in the learned sequence. In RP and RK matrices diagonal cells index pattern similarity in activation patterns between the same temporal position irrespective of finger movement and the same finger movement irrespective of position, respectively. **(B)** Group average neural similarity matrices for each ROI. In both panels, colour bars represent mean similarity (r). Note that color scales are different across matrices.

Finger-position binding in a motor sequence

To investigate whether ROIs support the binding between finger movements and their learned temporal position in the sequence, we computed similarity in activation patterns between individual finger movements across repetitions of the motor sequence. This resulted in an 8x8 neural similarity matrix for each ROI (i.e., Sequence (SEQ) matrix; Fig. 2). Analysis of the ***SEQ matrix*** revealed significantly higher mean similarity along the diagonal (i.e., same finger + position) as compared to the off-diagonal (i.e., different finger + position) in all ROIs (paired sample t-test: diagonal SEQ vs. off-diagonal SEQ; hippocampus, $t_{32} = 4.10$, $p_{FDR} < .001$; caudate, $t_{32} = 3.93$, $p < .001$; putamen, $t_{32} = 5.22$, $p_{FDR} < .001$; aSPL, $t_{32} = 9.41$, $p_{FDR} < .001$; SMA, $t_{32} = 8.581$, $p_{FDR} < .001$; PMC, $t_{32} = 13.74$, $p_{FDR} < .001$; M1, $t_{32} = 18.75$, $p_{FDR} < .001$; Fig. 3). These results suggest that activity patterns in all ROIs carry information about the binding between finger movements and their learned temporal position in the sequence. Importantly, as each finger movement in the sequence is bound to a specific position, both position and finger information are represented along the diagonal of the SEQ matrix. Accordingly, increased pattern similarity along the diagonal could be due to an overlap in either type of information. Control analyses were therefore performed using the random data to independently assess finger and position coding in our ROIs and estimate the contribution of these different processes to the similarity effects observed in the SEQ condition.

Finger and position coding in random movement patterns

To assess finger coding irrespective of serial position, we quantified pattern similarity in the RND condition between repetitions of the same as well as different finger movements (i.e., key presses; Random Key (RK) matrix; Fig. 2). Consistent with a pattern of finger coding, analysis of the ***RK matrix*** showed that mean similarity on the diagonal (i.e., same finger) was significantly higher as compared to the off-diagonal (i.e., different finger) in M1, PMC, SMA, aSPL and putamen (M1, $t_{32} = 22.85$, $p_{FDR} < .001$; PMC, $t_{32} = 9.97$, $p_{FDR} < .001$; SMA, $t_{32} = 5.38$, $p_{FDR} < .001$; aSPL, $t_{32} = 6.212$, $p_{FDR} = .003$; putamen, $t_{32} = 2.56$, $p_{FDR} = .009$; paired sample t-test: diagonal RK vs. off-diagonal RK; Fig. 3). Exploratory follow-up analyses furthermore revealed higher similarity between different fingers belonging to the same as compared to different hands in these regions, which corresponds to a pattern consistent with hand coding (all $t_{32} > 3.3$, all $p_{FDR} < .05$; paired sample t-test: within-hand RK vs. between-hand RK; see methods for details). Note that within M1, aSPL, PMC and SMA, our results support the presence of finger coding beyond hand coding (M1, $t_{32} = 13>256$, $p_{FDR} < .001$; PMC, $t_{32} = 4.617$, $p_{FDR} < .001$; SMA, $t_{32} = 1.682$, $p_{FDR} = .091$; aSPL, $t_{32} = 4.55$, $p_{FDR} < .001$; paired sample t-test: within-hand diagonal RK vs. within-hand off-diagonal RK). No evidence of finger coding was found in the hippocampus ($t_{32} = .489$, $p_{FDR} = .314$) and caudate ($t_{32} = 1.25$, $p_{FDR} = .122$). In summary, these findings

indicate that similarity effects in the SEQ condition in cortical ROIs and in the putamen might at least in part be attributed to finger and/or hand coding.

To assess position coding, we computed pattern similarity between different finger movements sharing the same temporal position as well as between different finger movements in different temporal positions in the RND task condition (Random Position (RP) matrix; Fig. 2). Analysis of the ***RP matrix*** indicated that mean similarity was significantly higher for the diagonal (i.e., same position) as compared to the off-diagonal (i.e., different position) for all ROIs with the exception of the hippocampus (paired sample t-test: diagonal RP vs. off-diagonal RP; hippocampus, t_{32} = .919, p_{FDR} = .191; caudate, t_{32} = 3.03, p_{FDR} = .003; putamen, t_{32} = 4.2 p_{FDR} < .001; aSPL, t_{32}= 5.44, p_{FDR} <.001; SMA, t_{32} = 3.818, p_{FDR} < .001; PMC, t_{32} = 10.77, p_{FDR} < .001; M1, t_{32} = 5.67, p_{FDR} < .001; Fig. 3). These results suggest that in these ROIs the increased similarity in the diagonal cells of the SEQ matrix might at least in part be attributed to position coding (but see below for follow-up analyses examining how higher similarity on positions 1 and 8 might account for these results in some ROIs).

Altogether, these analyses indicate that hippocampal patterns carry information about finger movements in their learned temporal position in the sequence condition (i.e., finger-position binding), but not about finger movements or positions in the random condition. In contrast, other ROIs showed evidence of finger-position coding in the sequence condition as well as position (caudate, putamen, M1, SMA, PMC and aSPL; but see temporal position analyses below) and finger/hand (putamen, M1, SMA, PMC and aSPL) coding during random practice.

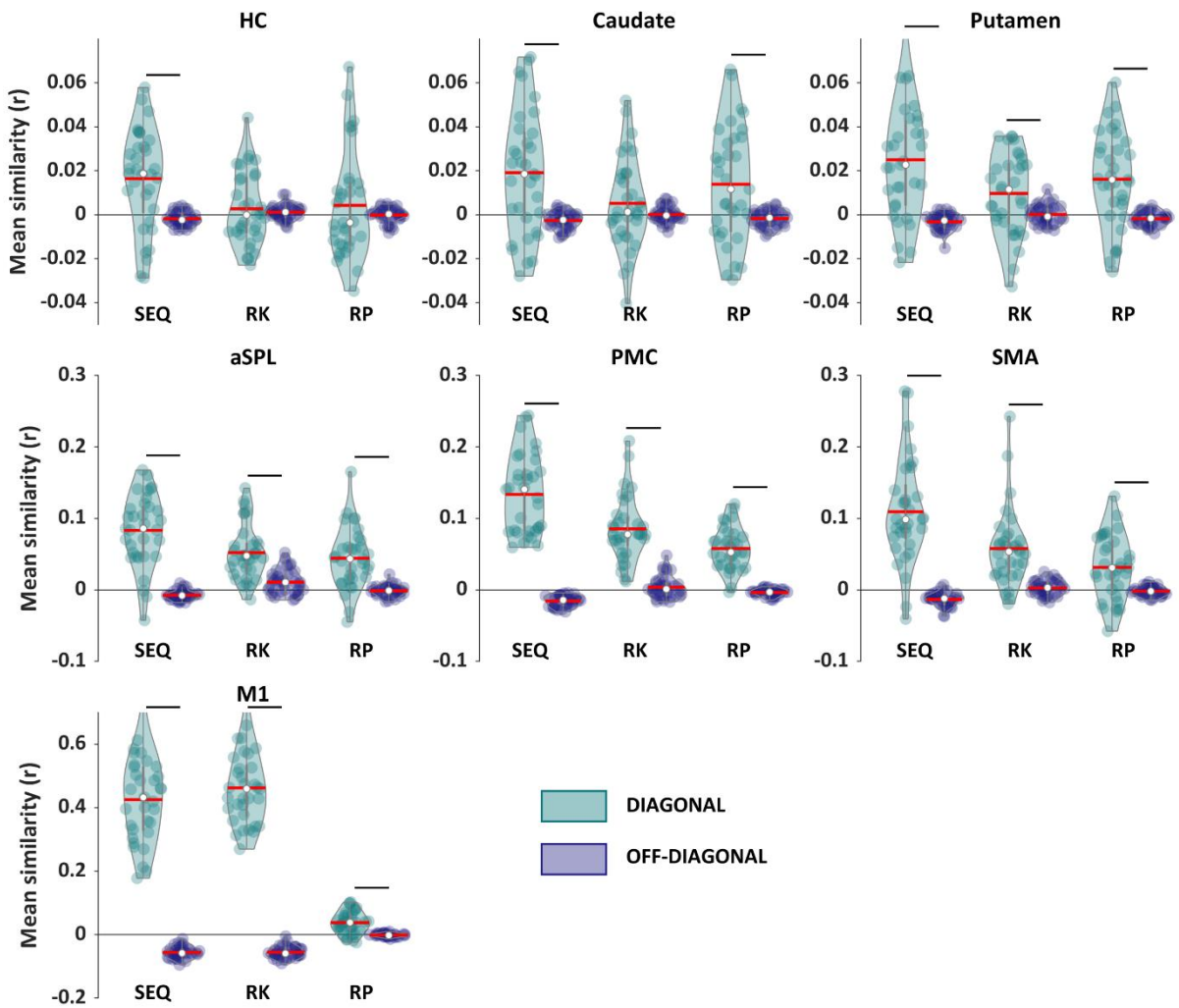

Figure 3. For each ROI, mean pattern similarity for diagonal and off-diagonal cells in the within-condition matrices was computed. If a particular ROI codes for a particular type of information, we expect higher similarity between trials sharing this information (i.e., diagonal) as compared to trials not sharing this information (i.e., off-diagonal). The hippocampus shows evidence for finger + position coding in the SEQ condition but not for finger or position coding in the random condition. In contrast, other ROIs showed evidence of finger-position coding in the sequence condition as well as position (caudate, putamen, M1, SMA, PMC and aSPL; but see temporal position analyses) and finger (putamen, M1, SMA, PMC and aSPL) coding during random practice. Coloured circles represent individual data, jittered in arbitrary distances on the x-axis to increase perceptibility. Red horizontal lines represent means and white circles represent medians. Black horizontal lines indicate significant differences between diagonal and off-diagonal (one sided paired sample t-test) at p_{FDR}<.05.

Pattern similarity as a function of temporal position

Inspection of the SEQ and RND Position similarity matrices suggest that, in some regions, the increased pattern similarity along the diagonal highlighted in the previous analyses are not homogenous across serial positions but are driven by the boundaries of the 8-element pattern (i.e., higher similarity on positions 1 and 8; Fig. 2B and see Supplementary Results section 1.2 for corresponding statistical analyses). To verify whether the binding and position coding effects reported in the previous section are driven by these boundary effects, we excluded boundary positions from

SEQ and RP matrices and reran the corresponding analyses. These control analyses showed that pattern similarity effects in the SEQ condition (same finger + position > different finger + position) remained significant in all ROIs, while there is no longer evidence that activation patterns in the caudate, putamen, M1, aSPL and SMA carry information about serial positions (other than boundary positions) in the random condition. The comparison in the random condition remained significant in PMC (p_{FDR}=.011). In sum, these analyses confirm that all ROIs show finger-position coding beyond boundaries in the sequence condition. They also refine the classification described above and indicate that only the PMC carries information about positions (other than boundaries) under random conditions. Altogether, these results indicate that hippocampal and caudate activation patterns carry information about finger-position binding but not about individual finger movements or positions in the random condition. In contrast, other ROIs showed evidence of binding in the sequence condition as well as finger (putamen, SMA, PMC and aSPL) and position (PMC) coding during random practice. These conclusions are summarized in Table 1 (the within-condition results presented above correspond to SEQ and RND rows of the table).

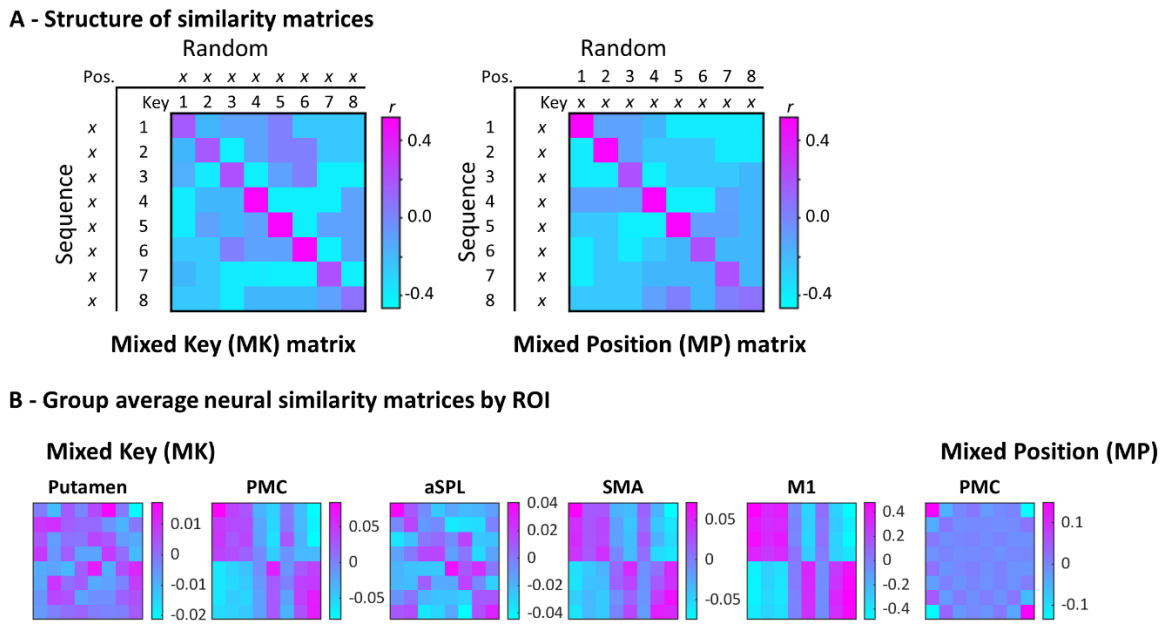

Figure 4. (A) Structure of mixed neural similarity matrices. Pattern similarity was computed across sequence and random task conditions to quantify whether finger (Mixed Key (MK) matrix) and position (Mixed Position (MP) matrix) coding was similar across conditions. In the MK matrix, diagonal cells index average similarity between the same finger movements across task conditions, while off-diagonal cells reflect average similarity across different finger movements. In the MP matrix, diagonal cells index average similarity between trials sharing the same serial position across sequence and random conditions, while off-diagonal cells reflect average similarity across different serial positions. **(B)** Group average mixed neural similarity matrices for ROIs that showed finger and/or position coding (after controlling for boundaries) under random task conditions. In both panels, colour bars represent mean similarity (r). Note that color scales are different across matrices.

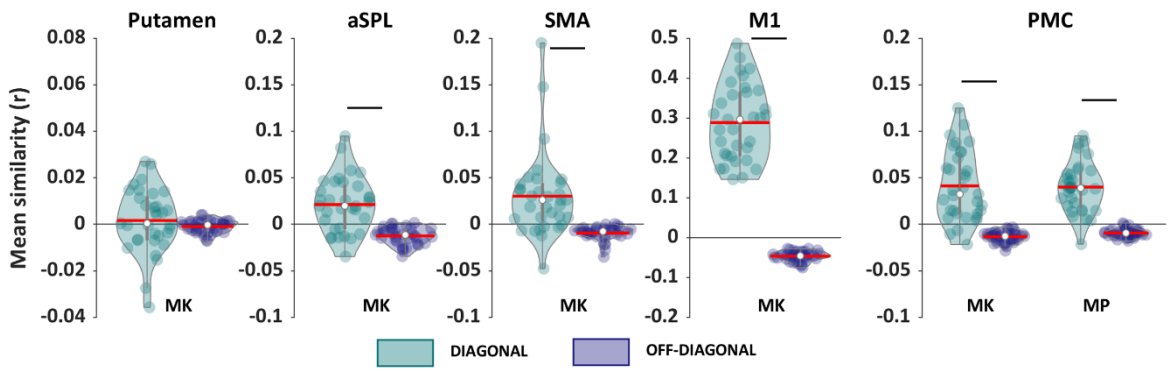

Figure 5. For ROIs that showed finger and/or position coding under random task conditions, mean pattern similarity for diagonal (green) and off-diagonal (purple) cells in the Mixed Key (MK) and Position (MP) similarity matrices was compared. Results show that cortical regions (M1, SMA, aSPL and PMC) code for movement-based information similarly between sequence and random conditions, while the putamen does not show similar coding for finger movements across task conditions. In addition, PMC showed similar coding of position information across task conditions. Colored circles represent individual data, jittered in arbitrary distances on the x-axis to increase perceptibility. Red horizontal lines represent means and white circles represent medians. Black horizontal indicate significant differences between diagonal and off-diagonal (one-tailed paired sample t-test) at p_{FDR}<.05

Position and finger coding between conditions

Our results suggest that the increased pattern similarity observed along the diagonal of the SEQ matrix might be attributed to different processes in different ROIs (i.e., finger-position binding, finger and/or position coding). However, given the nature of the task, pure finger and position coding was assessed based on the random data and hence it remains unclear whether the finger and position coding as observed during random practice is similar during sequence practice. Accordingly, we designed two additional neural similarity matrices and quantified the similarity of finger and position coding between task conditions for ROIs showing finger and/or position coding (after controlling for boundaries) under random conditions (see Fig. 4A and 4B for the structure and group average mixed neural similarity matrices, respectively). If position and/or finger coding is similar across task conditions, one would expect that the same positions or finger movements, but embedded in different task conditions, would exhibit similar activation patterns. Analysis of the ***Mixed Key (MK) matrix*** showed that mean similarity on the diagonal (i.e., same finger) in M1 (t_{32} = 18.114, p_{FDR} < .001), PMC (t_{32} = 8.023, p_{FDR} < .001), SMA (t_{32} = 4.433, p_{FDR} < .001) and aSPL (t_{32}= 6.074, p_{FDR} <.001) was significantly higher as compared to the off-diagonal (i.e., different finger), while no differences between diagonal and off-diagonal were found in the putamen (t_{32} = .919, p_{FDR} = .213; paired sample t-test: diagonal MK vs. off-diagonal MK; Fig. 5). These results indicate that finger coding was similar between task conditions in the cortical ROIs. Analysis of the ***Mixed Position (MP) matrix*** indicated that mean similarity in the PMC was significantly higher for the diagonal (i.e., same position) as compared to the

off-diagonal (i.e., different position; paired sample t-test: diagonal MP vs. off-diagonal MP; $t_{32} = 9.354$, $p_{FDR} < .001$; Fig. 5), suggesting similar position coding between task conditions in this region. To verify whether MP similarity effects in the PMC are driven by the boundary effects reported above, we removed the boundary positions and reran the analysis. The comparisons remained significant, suggesting that coding of positions (other than boundaries) in the PMC is shared between task conditions. These conclusions are summarized in Table 1 (the between-condition results presented above correspond to RND+SEQ rows of the table).

Taken together with the SEQ results presented above (see Table 1 for a general summary), these analyses suggest that: (1) in M1, SMA and aSPL, finger coding contributed to the increased pattern similarity observed along the diagonal of the SEQ matrix, (2) in PMC, both position and finger coding contributed to the SEQ results and, (3) in the hippocampus and striatal regions (putamen and caudate), the increased similarity for same finger + position in the SEQ condition is due to finger-position binding rather than an overlap in either finger or position representation.

Table 1. Schematic overview of the neuroimaging results.

		Regions of interest						
Coding	**Condition**	HC	Caudate	Putamen	M1	SMA	aSPL	PMC
Finger+position	**SEQ**	✓	✓	✓	✓	✓	✓	✓
	w/o boundaries	✓	✓	✓	✓	✓	✓	✓
Finger	**RND**	✗	✗	✓	✓	✓	✓	✓
	RND+SEQ			✗	✓	✓	✓	✓
Position	**RND**	✗	✓	✓	✓	✓	✓	✓
	w/o boundaries	✗	✗	✗	✗	✗	✗	✓
	RND+SEQ							✓
	w/o boundaries							✓

Notes. Results of the within-condition analyses are presented in the SEQ and RND rows while between-condition analyses correspond to the RND+SEQ rows. Boundaries refer to boundary positions 1 and 8 in an 8-element movement pattern. w/o = without.

Discussion

In the current study, we used multivoxel pattern similarity analysis of fMRI data to unravel the brain processes supporting movement-position binding during motor sequence practice. In line with our hypothesis, we found that hippocampal multivoxel activation patterns specifically carried information about finger movements in their learned temporal position in the sequence (i.e., finger-position binding). Interestingly, a similar pattern of results was observed in the striatum. In contrast, cortical regions showed different coding profiles. Specifically, multivoxel patterns in M1, SMA and aSPL carried movement-based information while the PMC represented both movement- and position-based information during motor sequence practice.

Our analyses demonstrated that the hippocampus coded for finger movements in their learned temporal position in the sequence but not for movements or positions *per se*. These data suggest that the hippocampus supports the binding between movements and their ordinal position in the sequence and thus the encoding of temporal order in the learned sequence. Our results are in line with a recent fMRI study showing that hippocampal multivoxel patterns differentiate between motor sequences based on the order of movements (12). More strikingly, the present findings concur with studies in the non-motor domain demonstrating that the hippocampus encodes the temporal order of objects (4) and auditory stimuli (3) during sequence learning. It is therefore tempting to speculate that the hippocampus processes temporal order information during sequence learning irrespective of the nature of the items (e.g., objects, sounds, movements) and the type of memory (i.e., motor or non-motor). Based on earlier work in the motor domain showing that the hippocampus supports goal-based or spatial representations of motor sequences that are effector-independent (8), we hypothesize that hippocampal binding processes might support the encoding of the temporal order of response goals or spatial targets in the learned sequence. Interestingly, such an associative map linking response goals to their ordinal position in the sequence was proposed to serve as a cognitive framework that can be abstracted during motor sequence learning and subsequently used as a cognitive-motor schema in which new movements can be rapidly integrated (11). In summary, our findings add to the growing body of literature associating hippocampal function to motor sequence learning (e.g., (8, 9, 12, 17, 18)) and indicate that the hippocampus represents temporal order information about motor sequences. They also suggest that the ability of the hippocampus to encode temporal order during sequence learning might be a general process that is shared across memory systems. This explanation, however, remains to be specifically tested.

A pattern of results corresponding to movement-position binding was also observed in the striatum (putamen and caudate nucleus). These findings are consistent with recent work showing that the execution of different motor sequences consisting of the same finger movements, but in a different

order elicited distinct activation patterns in the striatum (12, 13). While these patterns of results appear to be similar in the hippocampus and the striatum, we suggest that they support different processes. Specifically, the ability of the striatum to bind movements to their temporal position in a sequence might be related to its well-described role in the formation of stimulus-response associations (19–21). The striatum is indeed known to learn probabilistic or predictive associations between stimuli and responses, and/or between motor responses in a sequence (19, 22). The current data suggest that the striatum encoded the association between specific movements and their position in the learned deterministic sequence. Interestingly, our data also show that the putamen carried effector-specific information during random task practice. Based on these observations and evidence from the literature that striatal responses support an effector-dependent, motoric representation of the sequence during learning (20, 21, 23), we argue that the striatal binding process might be movement-specific rather than goal-based as proposed for the hippocampus. Given the rigid nature of stimulus-response associations learned by the putamen (22), we also speculate that the finger-position map developed in the striatum is less susceptible to be abstracted as compared to the hippocampal binding map described above. However, these statements are speculative and warrant further investigation.

Our data further indicate that the contribution of cortical regions such as the primary motor cortex (M1), premotor (PMC), supplementary motor (SMA) and parietal (aSPL) regions to motor sequence learning might be attributed - at least in part - to movement coding. The results observed in M1 are consistent with earlier multivariate fMRI studies showing that M1 activation patterns relate to the execution of individual movements during motor sequence learning (14, 15). Importantly, our data demonstrate that movement-based information is not uniquely represented in the primary motor cortex during motor sequence learning but also in secondary motor areas (PMC and SMA) and parietal cortex (aSPL). This is in contradiction with earlier work showing that the premotor, supplementary motor and parietal regions encode the sequential context rather than individual movement components (13–15) but see (14) where no clear evidence for sequence representations was found in SMA). However, it is worth noting that while our analyses suggest a contribution via movement coding, they do not allow us to conclude that these regions do *not* code for finger-position binding during motor sequence learning (and hence do not represent sequence order). It is therefore possible that these cortical areas code for both binding and individual movements. Yet, we argue that the predominant movement coding observed in the cortical ROIs in our research - in contrast to earlier work - might be attributed to differences in learning stages between studies. Whereas participants were extensively trained (up to 5 days) before the scanning session in previous work (13–15), participants only completed one hour of training in the current study. Taken together with evidence that sequence-specific activation patterns in secondary areas show less stability early in learning (13) and that the ability to discriminate between new sequences is significantly lower than between

consolidated sequences in these areas (12), it could be argued that secondary motor and associative areas support individual movement representations early during learning while sequence representations - and therefore movement-position binding - might emerge at later learning stages.

In addition to the movement coding discussed above, the premotor cortex showed a profile consistent with position coding irrespective of task condition in the current study. Based on previous literature suggesting that the premotor cortex plays a key role in motor planning and action selection (e.g., (24–26)), it is tempting to speculate that position-specific multivoxel activation patterns in the PMC reflect action planning, i.e., the plan to complete a series of eight movements. However, as our analyses did not focus on this preparatory period, this interpretation needs to be made with caution. Nevertheless, we argue that PMC position patterns might reflect the availability of a temporal scaffold (here of eight elements) within which movements will be implemented. Such an interpretation is in line with prior research showing that the premotor cortex encodes temporal features about motor sequences (e.g., interval between key presses) irrespective of the movements performed (27). It is also in line with animal work indicating that PMC neurons are not only tuned to interval duration but also to specific positions in a series of movements (28). Although the implementation of such a position framework seems especially important to efficiently prepare and implement responses in the sequence task, similar position coding processes were observed during random practice. It is possible that the visual cues indicating the ordinal position of movements in the 8-element stream (see Fig. S1) might have triggered the development of a similar framework in the random condition. Last and as above, we cannot rule out that the premotor cortex does not code for binding and it is therefore possible that multiple representations are available in the premotor cortex, as described in earlier research (27).

Lastly, in all our ROIs, we found that pattern similarity was increased for boundary positions (i.e., positions 1 and 8) as compared to positions in the middle of the movement pattern in both task conditions. It is possible that the perception of boundaries was facilitated by the visual cues indicating the ordinal position of movements in the 8-element stream (i.e., asterisks on the top of the screen indicating the progress within the 8-element movement pattern; Fig. S1). As these effects were observed in both the sequence and random tasks, we speculate that they might, at least in part, be driven by general attentional processes. Consistent with this idea, evidence in the non-motor domain shows that attentional states can modulate pattern similarity in cortical and subcortical regions (e.g., (29)). We suggest that attention was increased at the start and the end of the 8-element stream (i.e., either to adapt to/recognize the new condition or to prepare for a possible condition switch), which in turn modulated pattern similarity at these boundary positions. Finally, it seems possible that the lack of position and/or movement coding in the hippocampus is due to a generally lower signal-to-noise

ratio in subcortical regions. However, given that there was evidence for effector and position (boundary) coding in striatal regions, this seems unlikely.

In summary, the present results demonstrate that both the hippocampus and the striatum represent information about movements in their learned position in the sequence and hence encode the temporal order of movements. We propose that these regions might bind different representations, i.e., response goals in the hippocampus as opposed to motor responses in the striatum, to their ordinal position in the sequence. Our data also refine the functional role of motor cortical (M1, SMA, PMC) and parietal regions (aSPL) in motor sequence learning and indicate a contribution through movement and position coding. Altogether, our results do not only provide novel insight into the role of the hippocampus in the procedural memory domain but also deepen our understanding of the involvement of striatal and cortical regions in motor sequence learning.

Material and methods

Participants

The study was approved by the Medical Ethics Committee of the University Hospital Leuven, Belgium (B322201525025). Thirty-five healthy, young (mean age: 23.4, range: 19-29, 20 females), right-handed (Edinburgh Handedness questionnaire; (30)) adults were recruited to participate in the study. All participants provided written informed consent at the start of the study. They did not report any current or previous neurological or psychiatric diseases and were free of medications. None of the participants were musicians or professional typists. Based on standardized questionnaires, participants exhibited no indication of anxiety (Beck Anxiety Inventory; (32)) or depression (Beck Depression Inventory; (33)). All participants reported normal sleep quality and quantity during the month prior to the study, as evaluated with the Pittsburgh Sleep Quality Index (34). Two participants were excluded from further analyses: one due to brain abnormality and in one participant the fMRI session was aborted prior to completion due to severe anxiety during scanning. A total of 33 participants (19 females) were considered for the analyses. Participant characteristics can be found in Supplementary Table S1. Note that data of fMRI run 8 for one participant and data of the retention test for another participant are missing.

General experimental procedure

The experimental procedure is depicted in Figure 1. Participants were instructed to respect a regular sleep/wake schedule (according to their own schedule ± 1 hour) starting three days before the experimental session. Compliance to this schedule was assessed using sleep diaries (sleep measures are reported in Supplementary Table 1). Consumption of alcohol, nicotine, and caffeine (and other

vigilance-altering substances) was prohibited the day before as well as the day of the experimental session. The St. Mary's Hospital Sleep Questionnaire (35) was used to assess subjective sleep quality of the night before the experimental session (Supplementary Table 1). During the experimental session, participants performed different versions of an explicit serial reaction time task (SRTT; see details below and Fig. S1; (36)). After baseline assessment of motor performance using a random SRTT, participants were trained on a sequential SRTT during which they learned a sequence of eight finger movements through repeated practice (learning session, duration: 60 min., Fig. 1A). Immediately following the learning phase, participants were placed in the MRI scanner where they performed the pre-trained sequential SRTT, as well as a random SRTT (fMRI session, duration: 60min, Fig. 1A). Last, immediately after the fMRI session, all participants completed a retention test outside the scanner (retention, duration: 10min, Fig. 1A). Both learning and retention phases took place in a behavioral testing room in the vicinity of the MRI scanner.

Serial Reaction Time task and behavioural measures

We used an explicit bimanual serial reaction time task that was implemented in Matlab Psychophysics Toolbox version 3 (37). During the task, eight squares were presented on the screen, each corresponding to one of eight keys on the keyboard and one of eight fingers (no thumbs; Fig. S1). The outline of the squares alternated between red and green, indicating rest and practice, respectively. During rest, participants were instructed to keep their eyes focused on the screen and their fingers still on the keyboard (duration: 10s). During practice, the outline of the squares turned green, and participants were instructed to press as quickly and accurately as possible the key corresponding to the location of a cue (green filled square) that appeared on the screen. After a response, the next cue appeared (jittered response to stimulus interval, range: 1.5-2.5s, average 2s). Depending on the task condition, the cues either followed a pseudorandom (RND; motor control task) or a fixed, repeating sequential pattern (SEQ; motor sequence learning task). In the SEQ condition, participants repeatedly practiced a pre-determined eight-element sequence in which each finger had to be pressed once (4-7-3-8-6-2-5-1, with 1 and 8 corresponding to the little fingers of the left and right hand, respectively). All participants were trained on the same sequence of movements. However, to optimize the fMRI multivariate pattern analysis (see below), the starting point of the sequence was counterbalanced across participants such that the same key was not associated to the same temporal position in a sequence across individuals (i.e., the sequence started with 4 in participant 1, with 7 in participant 2, etc.). In the RND task condition, there was no repeating sequence, but each finger had to be pressed once every eight elements. During practice of both the random and sequential SRTT, the serial position of a trial in a stream of eight elements was indicated by a green asterisk on top of the screen (Fig. S1). These asterisks were replaced by eight red asterisks at rest.

At the beginning of the study, participants were informed that the cues could either follow a random or a repeating sequential pattern. During learning and retention, task practice took place outside the scanner, on a computer keyboard sitting at a desk, and was organized in blocks consisting of 48 keypresses each [which corresponded to six repetitions of the fixed sequence or six consecutive pseudo-random series of eight key presses], alternated with 10s rest periods (block design). During the learning session, participants completed four blocks of RND practice, followed by 20 blocks of SEQ practice. The retention test took place immediately after the fMRI session described below and consisted of four SEQ blocks followed by four RND blocks. During the fMRI session, the task was performed on an MRI compatible keyboard. Brain and behavioral data were acquired over eight consecutive scanning runs. Each fMRI run included 6 repetitions of the 8-element learned sequence (SEQ condition) and 6 pseudo-random series of 8 key presses (RND condition); thus 12 8-element key series (i.e., 6 repetitions x 2 conditions x 8 keypresses = 96 key presses/run). Repetitions of the learned sequence were randomly alternated with random patterns with the rule that a specific condition was not presented more than two times in a row. Half of the runs started with the SEQ condition, and the other half with the RND condition. In addition, three 10s rest periods were randomly inserted between 8-element series repetitions within each run. For each block (learning and retention sessions) and run (fMRI session), performance speed and accuracy were computed for each condition as the mean response time for correct responses (ms) and the percentage of correct responses, respectively.

Statistical analyses of behavioral data

Statistical analyses on behavioral data were performed in SPSS Statistics 25 (IBM). To investigate behavioral changes during the learning session, for each task, a one-way RM ANOVA with block (4 for random, 20 for sequence) as within-subjects factor was performed on both speed and accuracy measures. Behavioral changes in speed and accuracy during both the fMRI and retention sessions were examined with a condition (2: sequence vs. random) by run (8) / block (4) RM ANOVA. In case of violation of the sphericity assumption, Greenhouse-Geisser corrections were applied.

fMRI data acquisition

Images were acquired with a Phillips Achieva 3.0T MRI System and a 32-channel head coil. During the eight task runs, BOLD signal was acquired with a T2* gradient echo-planar sequence using axial slice orientation that covers the whole brain (TR =2000 ms, TE=30 ms, FA= 90°, 54 transverse slices, 2.5 mm slice thickness, 0.2 mm inter-slice gap, FoV = 210 × 210 mm^2, matrix size = 84 × 82 × 54 slices, voxel size = 2.5 × 2.56 × 2.5 mm^3). A structural T1-weighted 3D MP-RAGE sequence (TR = 9.5 ms, TE = 4.6 ms, TI = 858.1 ms, FA = 9°, 160 slices, FoV = 250 × 250 mm^2, matrix size = 256 × 256 × 160,

voxel size = 0.98 × 0.98 × 1.20 mm^3) was also obtained for each participant during the same scanning session.

fMRI data analysis

Statistical parametric mapping (SPM12; Welcome Department of Imaging Neuroscience, London, UK) was used for preprocessing of functional images and statistical analyses of BOLD data. To compute neural similarity matrices (see Representational similarity analyses section) the CoSMoMVPA toolbox was used in Matlab (38). Statistical analyses on neural similarity data were performed in SPSS Statistics 25 (IBM).

Preprocessing

Preprocessing included slice time correction (reference: middle slice), realignment of functional time series (to first image of each run separately in a first step and to the across-run mean functional image in a second step), co-registration of the pre-processed functional images to the structural T1-image and segmentation of the anatomical image. All the *multivariate analyses* were performed in native space (without normalization) to optimally accommodate inter-individual variability in the topography of memory representations ((39). Data to be used in *univariate group analyses* were further spatially normalized to an MNI (Montreal Neurological Institute) template (resampling size of 2 x 2 x 2 mm) and spatially smoothed (functional images only, Gaussian kernel, 8 mm fullwidth at half-maximum [FWHM]).

Regions of interest

The goal of the fMRI analyses was to examine brain patterns elicited in specific regions of interest (ROIs) by sequence and random task practice. The following (bilateral) ROIs were selected *a priori* based on previous literature describing their critical involvement in motor sequence learning processes (e.g., (6, 13, 23)): the primary motor cortex (M1), the supplementary motor cortex (SMA), the premotor cortex (PMC), the anterior part of the superior parietal lobule (aSPL), the hippocampus, the putamen and the caudate nucleus. Cortical ROIs were functionally defined while sub-cortical ROIs were anatomically defined (e.g., (40–42)).

The univariate analysis of fMRI data performed to extract the cortical ROIs was conducted in two serial steps accounting for fixed and random effects, respectively. In the first-level fixed effects analysis, a general linear model (GLM) was fitted for each individual to the normalized smoothed functional data. For each run, neural responses to each cue (corresponding to a specific finger movement) in the SEQ and RND task conditions were modelled in two separate regressors using delta (stick) functions locked to the cue onset (duration 0ms, event-related design) and convolved with a canonical hemodynamic response function. Movement errors (i.e., incorrect key presses) as well as

key presses during rest were modelled as events of no interest. Movement parameters (derived from realignment of the functional volumes) were entered as regressors of no interest. High-pass filtering with a cut-off period of 128 s served to remove low-frequency drifts from the time series. An autoregressive (order 1) plus white noise model and a restricted maximum likelihood (ReML) algorithm was used to estimate serial correlations in fMRI signal. Single subject contrast maps obtained from this first-level analysis and testing for the main effect of practice across task conditions were further spatially smoothed (Gaussian kernel 6 mm FWHM) and entered into a second-level random effects analysis (one sample t-test; see Fig. S2 for results). Cortical ROIs were defined as the intersection between the one-sample t statistic map [SPM(T)], thresholded at $p < .0001$, uncorrected for multiple comparisons and an anatomical mask. Anatomical masks for SMA, PMC and M1 were extracted from the Human Motor Area Template (HMAT; (43)) while the masks for the aSPL (defined to include anterior, medial and ventral intraparietal sulcus) were extracted from the Julich-Brain atlas ((44). The resulting ROI masks were mapped back to individual native space using the individual's inverse deformation field output from the segmentation of the anatomical image. Subcortical ROIS (bilateral hippocampus, putamen and caudate) were anatomically defined in native space using FSL's automated subcortical segmentation protocol (FIRST; FMRIB Software Library, Oxford Centre for fMRI of the Brain, Oxford, UK). All ROIs were masked to exclude voxels outside of the brain and with <10% grey matter probability and registered to the functional volumes.

Representational similarity analyses

Representational similarity analyses (RSA) were designed to investigate coding of finger-position binding, position- and movement-based information within specific ROIs. As the finger-position assignment is not fixed in the random condition, RSA allow to identify ROIs coding for position (irrespective of finger movement) and finger movement (irrespective of their temporal position in the pattern). As finger movements are performed in a fixed order in the sequence condition, RSA identify ROIs coding for finger-position binding in the sequence. For the RSA, two separate GLMs were fitted to the preprocessed functional data in each subject's native space (i.e., functional images slice time-corrected, realigned and coregistered to the T1, see preprocessing section above). The first GLM (i.e., position GLM) included separate regressors for each temporal position (8 positions per movement pattern), separately for each condition (8 positions x 2 conditions = 16 regressors per run). A second GLM (i.e., key GLM) was constructed to model neural responses evoked by individual key presses (fingers 1 to 8). In this GLM, one regressor was included for each finger/key, separately for each condition (8 keys x 2 conditions = 16 regressors per run). Note that the finger-position association was fixed in the SEQ condition thus, the same events were modelled in the position and key GLMs. In the RND condition, the order of key presses to be made changed with every repetition, hence events were

classified according to temporal position (i.e., position in the series of eight key presses) for the position GLM and key press (irrespective of temporal position) for the key GLM. In both GLMs, neural responses to events of interest (i.e., temporal positions and key presses, respectively) were modelled with delta functions (0ms duration) time locked to cue onsets (6 events per regressor per run). Key presses during rest and movement parameters (derived from realignment of the functional volumes) were modelled and entered as regressors of no interest in both GLMs. High pass filtering and serial correlation estimation were similar as for the univariate analyses. These GLMs generated separate maps of t-values for each regressor in each run and for each voxel of each ROI. This allowed the extraction of one across-voxel vector of t-values per regressor, run and ROI for each individual. For each voxel within each ROI, t-values were normalized by subtracting the mean t-value across all regressors (vectors) for each run separately. As GLMs 1 and 2 included identical regressors for the SEQ condition, corresponding vectors were averaged.

Next, neural similarity matrices were estimated for each ROI by computing the Pearson correlation coefficient between vectors of t-values. To do so, the full dataset (8 runs) was randomly divided into two independent subsets of 4 runs (using randperm function in Matlab). For each condition, vectors of t-values were then averaged across the 4 runs within the 2 separate subsets of runs and the resulting values were then correlated between the two datasets. This procedure was repeated 100 times (39, 45, 46) and correlations were then averaged across the 100 iterations, thus resulting in an 8 x 8 correlation matrix for each participant, ROI and research question of interest (see below). A total of five matrices were built to address the different research questions. As illustrated in Figure 2A, three within-condition matrices were created. (1) The SEQ matrix represents pattern similarity across repetitions of the motor sequence and was used to examine brain patterns coding for the binding between finger and position in the SEQ condition. (2) The Random Position (RP) matrix represents pattern similarity across repetitions of the random patterns and was designed to examine coding for temporal position irrespective of finger movement in the RND condition. (3) The Random Key (RK) matrix was built by computing pattern similarity in the RND condition between repetitions of the same finger movement and was used to highlight coding of finger movements irrespective of their temporal position. Last, and as illustrated in Figure 4A, two “mixed’ matrices presented similarity across SEQ and RND conditions to investigate (4) similarity of position (Mixed Position (MP) matrix) and (5) movement (Mixed Key (MK) matrix) coding between task conditions. All correlations were Fisher-transformed before entering statistical analyses.

Statistical analyses

To investigate whether a given area coded for a particular type of information, we computed for each ROI and neural similarity matrix the mean correlation in the diagonal and non-diagonal cells

(16). Then, for each matrix, a (one-tailed) paired sample t-test was performed across participants to compare diagonal vs. non-diagonal mean similarity. As an exploratory follow-up analysis on the Random Key matrix, we assessed whether certain ROIs showed higher similarity between different fingers belonging to the same as compared to different hands, which would correspond to a pattern consistent with hand coding. To do so we compared for each ROI the mean correlation in the within-hand (upper left and lower right) and between-hand (lower left and upper right) quadrants of the RK matrix, while excluding cells on the primary and secondary diagonal of the matrix. To examine whether there was key beyond hand coding within the same hand, we compared the diagonal mean similarity with non-diagonal mean similarity, while excluding the between-hand quadrants. For each group of hypotheses, the False Discovery Rate (FDR) procedure was applied to correct for multiple testing (i.e., corrected for 7 ROIs x 3 matrices = 21 tests for within-condition and 7 ROIs x 2 matrices = 14 tests for mixed-condition). To examine whether similarity changed as a function of serial position in the RND or SEQ task conditions, we ran a condition by serial position RM ANOVA on diagonal similarity values in the SEQ and RP matrices for each ROI. Significant effects were followed up with planned pairwise comparisons and corrected for multiple comparisons using the FDR procedure (i.e., 7 comparisons per position = 7 tests). In case of violation of the sphericity assumption, Greenhouse-Geisser corrections were applied. The results of the RM ANOVAs are reported in Supplementary Material section 1.2 and Table S2.

Data and Code Availability

Source data for all figures and statistical analyses in SPSS are provided with this paper. The approval granted by the local ethics committee does not permit the sharing of individual neuroimaging data. However, individual behavioral and pattern similarity data as well as the scripts to process the data will be made freely available on Zenodo.

Funding. This work was supported by the Belgian Research Foundation Flanders (FWO; G099516N, 1524218N) and internal funds from KU Leuven. GA also received support from FWO (G0D7918N, G0B1419N) and Excellence of Science (EOS, 30446199, MEMODYN). ND received salary support from these grants and from the Belgian American Educational Fund (BAEF). SR is funded by a predoctoral fellowship from FWO (1141320N). HO received support from FWO (G0D3322N) and KU Leuven (C14/21/047).

Acknowlegments. We wish to thank Ather Mujitaba for assistance with data collection and Brendan Ritchie for his advise on multi-variate analyses of fMRI data.

References

1. L. Davachi, S. DuBrow, How the hippocampus preserves order: The role of prediction and context. *Trends Cogn Sci* **19**, 92–99 (2015).
2. Y. Ezzyat, L. Davachi, Similarity Breeds Proximity: Pattern Similarity within and across Contexts Is Related to Later Mnemonic Judgments of Temporal Proximity. *Neuron* **81**, 1179–1189 (2014).
3. K. Kalm, M. H. Davis, D. Norris, Individual Sequence Representations in the Medial Temporal Lobe. *J Cogn Neurosci* **25**, 111–1124 (2013).
4. L. T. Hsieh, M. J. Gruber, L. J. Jenkins, C. Ranganath, Hippocampal Activity Patterns Carry Information about Objects in Temporal Context. *Neuron* **81**, 1165–1178 (2014).
5. S. DuBrow, L. Davachi, Temporal memory is shaped by encoding stability and intervening item reactivation. *Journal of Neuroscience* **34**, 13998–14005 (2014).
6. G. Albouy, B. R. King, P. Maquet, J. Doyon, Hippocampus and striatum: Dynamics and interaction during acquisition and sleep-related motor sequence memory consolidation. *Hippocampus* **23**, 985–1004 (2013).
7. B. R. King, K. Hoedlmoser, F. Hirschauer, N. Dolfen, G. Albouy, Sleeping on the motor engram: The multifaceted nature of sleep-related motor memory consolidation. *Neurosci Biobehav Rev* **80**, 1–22 (2017).
8. G. Albouy, *et al.*, Maintaining vs. enhancing motor sequence memories: respective roles of striatal and hippocampal systems. *Neuroimage* **108**, 423–434 (2015).
9. B. R. King, M. A. Gann, D. Mantini, J. Doyon, G. Albouy, Persistence of hippocampal and striatal multivoxel patterns during awake rest after motor sequence learning. *iScience* **25**, 105498 (2022).
10. G. Albouy, *et al.*, Daytime Sleep Enhances Consolidation of the Spatial but Not Motoric Representation of Motor Sequence Memory. *PLoS One* **8** (2013).
11. B. R. King, *et al.*, Schema and Motor-Memory Consolidation. *Psychol Sci* **30**, 963–978 (2019).
12. B. Pinsard, *et al.*, Consolidation alters motor sequence- specific distributed representations. *Elife* **8**, 1–20 (2019).
13. E. Berlot, N. J. Popp, J. Diedrichsen, A critical re-evaluation of fmri signatures of motor sequence learning. *Elife* **9**, 1–24 (2020).
14. A. Yokoi, S. A. Arbuckle, J. Diedrichsen, The role of human primary motor cortex in the production of skilled finger sequences. *Journal of Neuroscience* **38**, 1430–1442 (2018).
15. A. Yokoi, J. Diedrichsen, Neural Organization of Hierarchical Motor Sequence Representations in the Human Neocortex. *Neuron* **103**, 1178-1190.e7 (2019).
16. N. Kriegeskorte, M. Mur, P. Bandettini, Representational similarity analysis - connecting the branches of systems neuroscience. *Front Syst Neurosci* **2**, 1–28 (2008).
17. F. Jacobacci, *et al.*, Rapid hippocampal plasticity supports motor sequence learning. *Proc Natl Acad Sci U S A* **117**, 23898–23903 (2020).
18. E. R. Buch, L. Claudino, R. Quentin, M. Bönstrup, L. G. Cohen, Consolidation of human skill linked to waking hippocampo-neocortical replay. *Cell Rep* **35**, 109193 (2021).
19. V. Penhune, C. J. Steele, Parallel contributions of cerebellar, striatal and M1 mechanisms to motor sequence learning. *Behavioural Brain Research* **226**, 579–591 (2012).
20. O. Hikosaka, *et al.*, Parallel neural networks for learning sequential procedures. *Trends Neurosci* **22**, 464–471 (1999).
21. O. Hikosaka, K. Nakamura, K. Sakai, H. Nakahara, Central mechanisms of motor skill learning. *Curr Opin Neurobiol* **12**, 217–222 (2002).
22. A. Graybiel, Habits, rituals, and the evaluative brain. *Annu Rev Neurosci* **31**, 359–387 (2008).
23. J. Doyon, V. Penhune, L. G. Ungerleider, Distinct contribution of the cortico-striatal and cortico-cerebellar systems to motor skill learning. *Neuropsychologia* **41**, 252–262 (2003).
24. S. T. Grafton, A. H. Fagg, M. A. Arbib, Dorsal premotor cortex and conditional movement selection: A PET functional mapping study. *J Neurophysiol* **79**, 1092–1097 (1998).

25. E. Hoshi, J. Tanji, Differential involvement of neurons in the dorsal and ventral premotor cortex during processing of visual signals for action planning. *J Neurophysiol* **95**, 3596–3616 (2006).
26. C. Cavina-Pratesi, *et al.*, Behavioral/Systems/Cognitive Dissociating Arbitrary Stimulus-Response Mapping from Movement Planning during Preparatory Period: Evidence from Event-Related Functional Magnetic Resonance Imaging (2006) https:/doi.org/10.1523/JNEUROSCI.3176-05.2006 (October 4, 2022).
27. K. Kornysheva, J. Diedrichsen, Human premotor areas parse sequences into their spatial and temporal features. *Elife* **3**, e03043 (2014).
28. H. Merchant, O. Pérez, W. Zarco, J. Gámez, Interval Tuning in the Primate Medial Premotor Cortex as a General Timing Mechanism. *Journal of Neuroscience* **33**, 9082–9096 (2013).
29. M. Aly, N. B. Turk-Browne, Attention promotes episodic encoding by stabilizing hippocampal representations. *Proc Natl Acad Sci U S A* **113**, E420–E429 (2016).
30. R. C. Oldfield, The assessment and analysis of handedness: The Edinburgh inventory. *Neuropsychologia* **9**, 97–113 (1971).
31. A. Beck, N. Epstein, G. Brown, R. Steer, An inventory for measuring clinical anxiety: psychometric properties. *J Consult Clin Psychol* **56**, 893–897 (1988).
32. A. Beck, N. Epstein, G. Brown, R. Steer, An inventory for measuring clinical anxiety: psychometric properties. *J Consult Clin Psychol* **56**, 893–897 (1988).
33. A. T. Beck, C. H. Ward, M. Mendelson, J. Mock, J. Erbaugh, An Inventory for Measuring Depression. *Arch Gen Psychiatry* **4**, 561–571 (1961).
34. D. J. Buysse, *et al.*, The Pittsburgh Sleep Quality Index: a new instrument for psychiatric practice and research. *Psychiatry Res* **28**, 193–213 (1989).
35. B. W. Ellis, *et al.*, The St . Mary ' s Hospital Sleep Questionnaire : A Study of Reliability. *Sleep* **4**, 93–97 (1981).
36. M. J. Nissen, P. Bullemer, Attentional requirements of learning: Evidence from performance measures. *Cogn Psychol* **19**, 1–32 (1987).
37. M. Kleiner, *et al.*, What's new in Psychtoolbox-3? *Perception* **36**, S14 (2007).
38. S. M. Plis, M. J. Rosa, N. N. Oosterhof, A. C. Connolly, J. V Haxby, CoSMoMVPA: Multi-Modal Multivariate Pattern Analysis of Neuroimaging Data in Matlab/GNU Octave. *Frontiers in Neuroinformatics | www.frontiersin.org* **1**, 27 (2016).
39. J. V. Haxby, *et al.*, Distributed and overlapping representations of faces and objects in ventral temporal corten. *Science (1979)* **293**, 87–96 (2001).
40. A. Tompary, L. Davachi, Consolidation Promotes the Emergence of Representational Overlap in the Hippocampus and Medial Prefrontal Cortex. *Neuron* **96**, 228-241.e5 (2017).
41. A. Tambini, M. D'Esposito, Causal Contribution of Awake Post-encoding Processes to Episodic Memory Consolidation. *Current Biology* **30**, 3533-3543.e7 (2020).
42. V. P. Murty, A. Tompary, R. A. Adcock, L. Davachi, Selectivity in postencoding connectivity with high-level visual cortex is associated with reward-motivated memory. *Journal of Neuroscience* **37**, 537–545 (2017).
43. M. A. Mayka, D. M. Corcos, S. E. Leurgans, D. E. Vaillancourt, Three-dimensional locations and boundaries of motor and premotor cortices as defined by functional brain imaging: A meta-analysis. *Neuroimage* **31**, 1453 (2006).
44. K. Amunts, H. Mohlberg, S. Bludau, K. Zilles, Julich-Brain: A 3D probabilistic atlas of the human brain's cytoarchitecture. *Science (1979)* **369**, 988–992 (2020).
45. H. P. Op De Beeck, K. Torfs, J. Wagemans, Perceived shape similarity among unfamiliar objects and the organization of the human object vision pathway. *Journal of Neuroscience* **28**, 10111–10123 (2008).
46. H. P. op de Beeck, M. Brants, A. Baeck, J. Wagemans, Distributed subordinate specificity for bodies, faces, and buildings in human ventral visual cortex. *Neuroimage* **49**, 3414–3425 (2010).